Tumor formation initiated by nondividing epidermal cells via an inflammatory infiltrate

Esther N. Arwert[a,1], Rohit Lal[b,1], Sven Quist[a], Ian Rosewell[c], Nico van Rooijen[d], and Fiona M. Watt[a,2]

[a]Cancer Research UK Cambridge Research Institute, Cambridge CB2 0RE, United Kingdom; [b]Department of Medical Oncology, Guy's and St. Thomas' Foundation Trust, Guy's Hospital, London SE1 9RT, United Kingdom; [c]Cancer Research UK Clare Hall Laboratories, South Mimms EN6 3LD, United Kingdom; and [d]Department of Molecular Cell Biology, Free University Medical Center, Amsterdam 1081 BT, The Netherlands

Edited by Charles A. Dinarello, University of Colorado Denver, Aurora, CO, and approved October 12, 2010 (received for review May 26, 2010)

In mammalian epidermis, integrin expression is normally confined to the basal proliferative layer that contains stem cells. However, in epidermal hyperproliferative disorders and tumors, integrins are also expressed by suprabasal cells, with concomitant up-regulation of Erk mitogen-activated protein kinase (MAPK) signaling. In transgenic mice, expression of activated MAPK kinase 1 (MEK1) in the suprabasal, nondividing, differentiated cell layers (InvEE transgenics) results in epidermal hyperproliferation and skin inflammation. We now demonstrate that wounding induces benign tumors (papillomas and keratoacanthomas) in InvEE mice. By generating chimeras between InvEE mice and mice that lack the MEK1 transgene, we demonstrate that differentiating, nondividing cells that express MEK1 stimulate adjacent transgene-negative cells to divide and become incorporated into the tumor mass. Dexamethasone treatment inhibits tumor formation, suggesting that inflammation is involved. InvEE skin and tumors express high levels of IL1α; treatment with an IL1 receptor antagonist delays tumor onset and reduces incidence. Depletion of γδ T cells and macrophages also reduces tumor incidence. Because a hallmark of cancer is uncontrolled proliferation, it is widely assumed that tumors arise only from dividing cells. In contrast, our studies show that differentiated epidermal cells can initiate tumor formation without reacquiring the ability to divide and that they do so by triggering an inflammatory infiltrate.

cancer | differentiation

Multilayered epithelia, such as the epidermis, comprise a basal layer of cells attached to an underlying basement membrane and suprabasal cells that undergo terminal differentiation as they move toward the surface of the tissue (1). Proliferating cells, including stem cells, are located in the basal layer and the onset of differentiation is associated with irreversible cell cycle exit.

Adhesion of basal cells to the basement membrane is mediated by integrin extracellular matrix receptors. Down-regulation of integrin function and expression links initiation of terminal differentiation to movement into the suprabasal layers (2). Altered integrin expression is a characteristic of tumors of multilayered epithelia and reflects both genetic and epigenetic changes (1, 3). One feature of human squamous cell carcinomas, which correlates with poor prognosis, is suprabasal integrin expression (1). Consistent with this, transgenic mice in which integrins are expressed above the basal layer can show increased susceptibility to chemically induced tumors (1).

Suprabasal β1 integrin expression, in both mice and humans, is associated with elevated Erk mitogen-activated protein kinase (MAPK) signaling and sporadic inflammation (4, 5). Transgenic mice that express constitutively active MEK1 in the suprabasal epidermal layers under the control of the involucrin promoter (InvEE transgenics) have hyperproliferative epidermis and a chronic inflammatory infiltrate (5). Conversely, loss of epidermal MEK1/2 greatly reduces proliferation (6).

Spontaneous papillomas develop in InvEE transgenics at sites of suspected injury or mechanical trauma (5). Because chronic inflammation can increase cancer risk and wounding can act as a tumor-promoting stimulus (7–9), we set out to investigate whether wounding is a sufficient stimulus for tumor development in InvEE mice and, if so, to explore the underlying mechanisms.

Results

Wounding Induces Benign Tumors in InvEE Transgenics. As previously reported, InvEE transgenics have a hyperproliferative epidermis and a chronic inflammatory infiltrate (Fig. 1 *A–D*). Spontaneous papillomas develop in the mice (Fig. 1 *E* and *F*) with a frequency of ≈9% (Fig. 1*G*) (5).

To examine whether wounding induces tumors, we made two 5-mm-diameter full thickness circular wounds in the back skin using a punch biopsy. As a result, ≈40% of mice developed papillomas (Fig. 1*G*). Most animals developed one tumor; 22% developed two. The incidence of tumors, whether spontaneous or wound-induced, was similar in males and females ($\chi^2 = 0.398$, $P = 0.528$ for spontaneous; $\chi^2 = 0.078$, $P = 0.780$ for wound-induced; Fig. 1*G*). Mice developed tumors 14–35 d after wounding (median = 21 d), regardless of age (Fig. 1*H*).

Tumors were examined 60 d after wounding, except when indicated. No littermate controls developed tumors. When monitored for longer than 60 d, InvEE papillomas did not regress, nor did they convert into malignant tumors. However, ≈10% underwent spontaneous conversion to keratoacanthomas, lesions that in human skin are regarded as low-grade squamous cell carcinomas (Fig. S1 *A–D*) (10).

Differentiating Transgene-Positive Cells Stimulate Proliferation of Basal Transgene-Negative Cells. In InvEE epidermis, proliferation is largely confined to the basal, transgene-negative layer in undamaged back skin (Fig. 1*D*), healing wounds (Fig. S1 *E* and *F*), and papillomas (5) (Fig. 1*F*). This implies that InvEE papillomas contain proliferating, transgene-negative cells. To confirm this, we made aggregate chimeras (GFP/InvEE) between embryos of InvEE mice and mice in which all cells express eGFP under the control of the CAGGS promoter (GFP transgenic mice).

In adult chimeric animals, GFP-positive and -negative regions were readily detected macroscopically and in histological sections (Fig. 2 *A–D*). We examined 16 spontaneous and wound-induced tumors in 12 InvEE chimeric mice. As controls, we generated 21 chimeras between GFP transgenic and wild-type embryos (GFP/WT), none of which developed spontaneous or wound-induced tumors. There was no evidence that the ratio of GFP-positive to GFP-negative epidermal regions differed between GFP/InvEE and GFP/WT chimeras.

Author contributions: E.N.A., R.L., and F.M.W. designed research; E.N.A. and R.L. performed research; S.Q., I.R., and N.v.R. contributed new reagents/analytic tools; E.N.A. and R.L. analyzed data; and E.N.A. and F.M.W. wrote the paper.

The authors declare no conflict of interest.

This article is a PNAS Direct Submission.

Freely available online through the PNAS open access option.

[1]E.N.A. and R.L. contributed equally to this work.

[2]To whom correspondence should be addressed. E-mail: fiona.watt@cancer.org.uk.

This article contains supporting information online at www.pnas.org/lookup/suppl/doi:10.1073/pnas.1007404107/-/DCSupplemental.

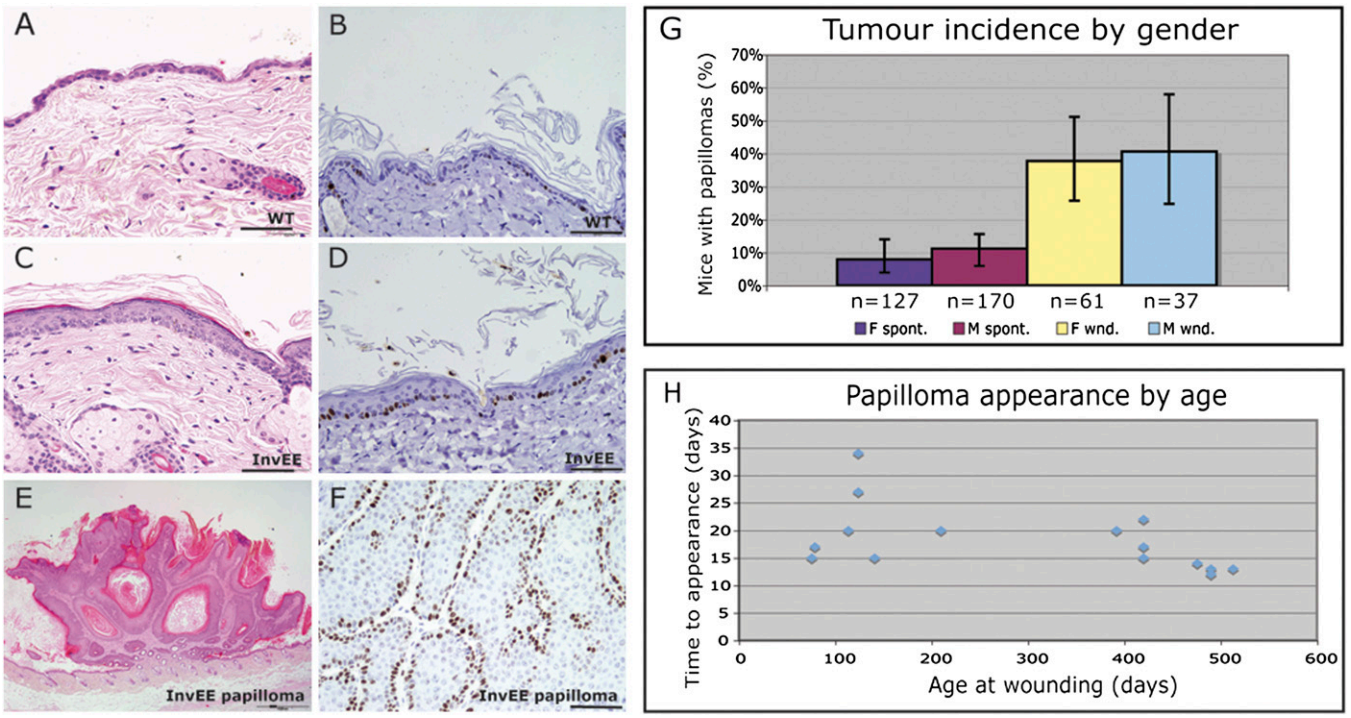

Fig. 1. Wound-induced papillomas in InvEE transgenic mice. (*A*, *C*, and *E*) H&E- and (*B*, *D*, and *F*) Ki67-stained sections of nontransgenic (WT: *A* and *B*) and InvEE transgenic (*C* and *D*) back skin and InvEE wound-induced papilloma (*E* and *F*). (Scale bar: 100 μm.) (*G*) Incidence of spontaneous ("spont": purple and mauve) and wound-induced ("wnd": yellow and blue) papillomas in male (M) and female (F) InvEE transgenic mice. Error bars: 95% confidence intervals. (*H*) Time between wounding and appearance of papillomas in InvEE mice of different ages.

Fourteen GFP/InvEE papillomas contained a substantial proportion of GFP-positive cells, which could be observed macroscopically or histologically (Fig. 2 *A–D* and Fig. S2 *A–C*, *G*, and *H*). In one papilloma, GFP-positive keratinocytes constituted less than 1% of the tumor, and in another papilloma, no GFP-positive cells were detected.

Sections of tumors were labeled with antibodies to Ki67, as a marker of proliferation; with antibodies to GFP to detect InvEE-negative regions; and with antibodies to the His tag on the MEK1 transgene to detect InvEE-positive regions (Fig. 2 *E* and *F*; Fig. S2 *D–F* and *H*). As additional markers of proliferation, antibodies to phospho-histone H3 or BrdU were also used (Fig. S2 *A–C*).

Within the His tag-positive regions, proliferation was confined to the transgene-negative basal cells underlying the differentiating MEK1-expressing layers, as observed previously in InvEE papillomas (5) (Fig. 2 *E* and *H* and orange arrows in *F*). Within GFP-positive regions, the GFP transgene was expressed by basal and suprabasal epidermal cells and also by cells in the underlying stroma; proliferating basal cells were therefore GFP positive (Fig. 2 *E* and *H* and pink arrows in *F*). No cells coexpressed GFP and His tag (Fig. 2 *E*, *F*, and *H*; Fig. S2 *D–F* and *H*). Suprabasal proliferative cells were rarely observed (Fig. 2 *E* and *F*; Fig. S2).

In GFP/WT chimeras, the rate of basal layer proliferation was the same in GFP-positive and -negative basal cells (Fig. 2 *G* and *H*). This was also the case in GFP/InvEE chimeras; however, the GFP-positive proliferation rate was higher than in GFP/WT chimeras ($t = 6.889$, $P = 0.001$), indicating that the presence of suprabasal MEK1-expressing cells stimulated proliferation in both the underlying GFP-negative basal cells and the adjacent GFP-positive basal cells (Fig. 2 *G* and *H*).

In InvEE/GFP papillomas, the proportion of GFP-negative proliferating basal cells was further increased ($t = 3.066$, $P = 0.0182$), but proliferation of GFP-positive cells did not increase as much (Fig. 2 *G* and *H*). The enhanced proliferation of basal cells was observed both when papillomas were first detectable (21 d, early papillomas; $n = 3$; Fig. S2*B*) and in well-established papillomas (60 d; $n = 11$; Fig. S2*C*). The ratio of Ki67-positive, GFP-negative to Ki67-positive, GFP-positive basal cells was 1.0 in InvEE chimeric skin, 1.1 in early papillomas, and 1.3 in late papillomas. Therefore, the proliferative advantage of GFP-negative basal cells was more apparent in late papillomas. We conclude that MEK1-expressing suprabasal cells stimulated proliferation of neighboring basal cells in both epidermis and papillomas, whether the basal cells were from InvEE epidermis or from adjacent GFP-positive epidermis.

Given the short time in which the papillomas developed, it is unlikely that the transgene-negative basal cells had acquired a significant burden of oncogenic mutations. In support of this, no mutations in the sequences of *Ha-Ras* [codon 12, 13, and 61 (11)] and *TP53* [exon 4–9 (12)] associated with epidermal tumors were found in nine of nine InvEE papillomas (four spontaneous, five wound-induced).

Role of IL1α. InvEE transgenic mice have a dermal inflammatory infiltrate (5), and wounding is known to induce inflammation in normal skin (13). Unwounded InvEE mice had enlarged spleens, and spleen weight was further increased in InvEE mice bearing papillomas, consistent with chronic inflammation (Fig. 3*A*).

Glucocorticoid anti-inflammatory drugs such as dexamethasone can prevent development of chemically induced mouse skin tumors and cause regression of human keratoacanthomas (10). We therefore examined the effects of treating mice with dexamethasone or cyclosporine A, two immunosuppressive agents that differ in their mode of action (Fig. 3*B*).

In cyclosporine A-treated animals ($n = 37$), the incidence and kinetics of wound-induced papilloma formation were indistinguishable from untreated controls ($n = 48$) ($\chi^2 = 0.0231$, $P = 0.8792$) (Fig. 3*B*). In contrast, during dexamethasone treatment none of the mice in the treatment group ($n = 50$) developed tumors (Fig. 3*B*). Thirty days after treatment 10% of dexametha-

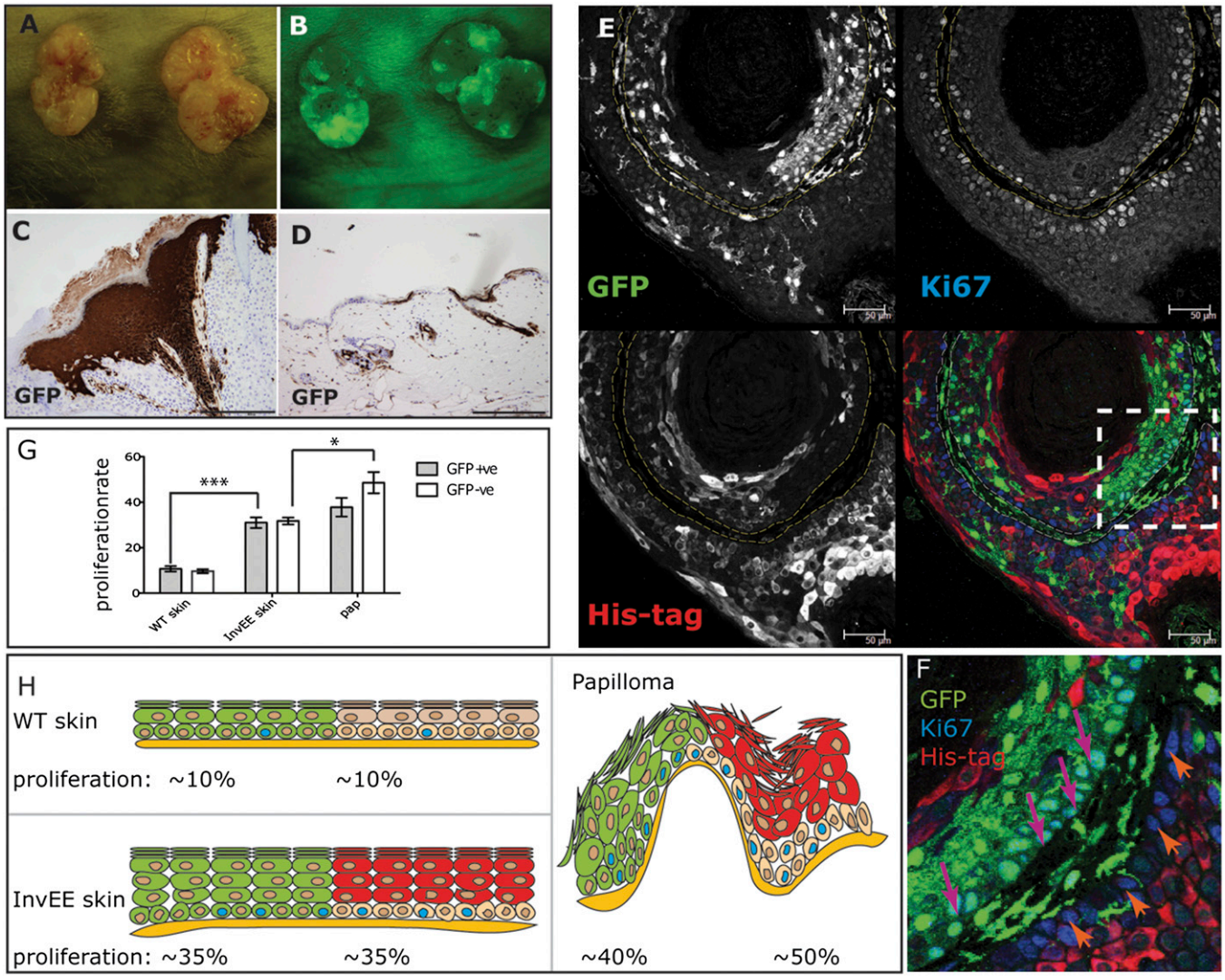

Fig. 2. Papilloma formation in GFP/InvEE chimeric mice. (*A* and *B*) Macroscopic appearance of two wound-induced papillomas, viewed under natural (*A*) and fluorescent (*B*) light. (*C* and *D*) GFP immunohistochemistry of papilloma (*C*) and skin (*D*) from GFP/InvEE mice. (*E* and *F*) GFP/InvEE papilloma labeled with antibodies to GFP (green), Ki67 (blue), and MEK1 transgene His tag (red). Each label is shown separately in black and white; merge is in color. Dashed lines in *E* demarcate basement membrane. (*F*) Enlarged view of boxed area in *E*, with GFP-negative, Ki67-positive basal cells indicated with orange arrows and GFP-positive, Ki67-positive cells indicated with pink arrows. [Scale bars: 200 μm (*C* and *D*); 50 μm (*E*).] (*G*) Percentage of GFP-positive (GFP+ve) or -negative (GFP-ve) basal cells that were Ki67 positive in GFP/WT skin (WT; $n = 3$), GFP/InvEE skin (InvEE skin; $n = 4$), and GFP/InvEE papillomas ("pap": $n = 4$). $^{*}P < 0.05$, $^{***}P < 0.001$. (*H*) Data in *G* shown schematically to illustrate relationship of GFP-positive (green) and -negative (beige) basal cells to the overlying suprabasal cells (GFP positive: green; GFP negative, MEK1 transgene positive: red).

sone-treated mice had developed tumors (Fig. 3*B*), a similar incidence to unwounded InvEE mice (Fig. 1*G*) and significantly lower than wounded mice that had received cyclosporine A ($\chi^2 = 21.994$, $P < 0.0001$). Dexamethasone treatment of preexisting tumors reduced tumor size in five of seven mice but did not cause complete regression (Fig. S3).

Inflammation in InvEE skin results, at least in part, from increased expression of IL-1α but not of IL-1β (4, 5). IL1α levels were further increased in InvEE papillomas (Fig. 3 *C* and *D*). Because dexamethasone decreases keratinocyte production of IL1α (14, 15), we tested whether blockade of IL1 with the IL1 receptor antagonist Kineret (16) would affect tumor formation (Fig. 3 *E* and *F*). Kineret treatment led to both a delay in tumor formation and a reduction in tumor burden (control $n = 29$, treatment $n = 36$; $\chi^2 = 7.53$, $P = 0.006$). We conclude that IL1α production contributes not only to enhanced proliferation of basal keratinocytes (5) but also to wound-induced tumor formation.

Role of γδT Cells and Macrophages. To investigate which bone marrow-derived cells contribute to wound-induced tumor formation, mice were sublethally irradiated and rescued by injection of either control (InvEE) bone marrow or bone marrow in which different cells had been ablated (Fig. 4*A*). The mice were allowed to recover for a minimum of 6 wk and then wounded. Tumor formation was monitored for at least 60 d after wounding. To confirm successful chimerism, male bone marrow was transplanted into female recipients and the spleen and skin of recipient mice were subjected to Y probe in situ hybridization (Fig. S4).

InvEE mice reconstituted with $Rag2^{-/-}$ bone marrow ($n = 23$), which lacks mature T and B cells (InvEE/$Rag2^{-/-}$), showed a significant reduction in tumor formation ($n = 42$; $\chi^2 = 9.36$, $P = 0.002$) (Fig. 4*B*). In contrast, mice reconstituted with T-cell receptor $\beta^{-/-}$ ($TCR\beta^{-/-}$) bone marrow ($n = 24$) developed the same number of tumors as controls; this indicates that αβ T cells did not contribute to tumor formation ($\chi^2 = 0.6$, $P = 0.44$) (Fig. 4*B*). Mice

CELL BIOLOGY

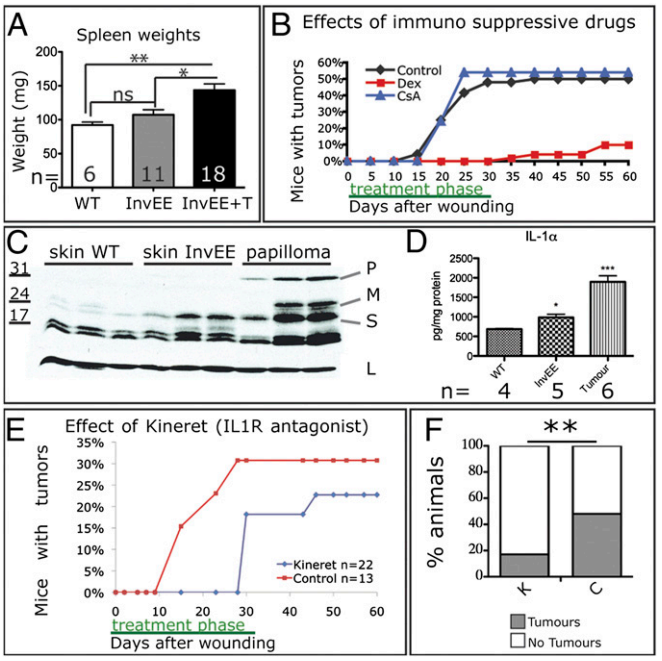

Fig. 3. Effect of IL1 on wound-induced tumor formation. (*A*) Spleen weights (mg) of wild type (WT), InvEE mice, and tumor-bearing InvEE mice (InvEE+T) with number of mice indicated. ns: not significant. (*B*) Effects of cyclosporine A and dexamethasone on wound-induced tumor formation. (*C*) Western blot of wild-type (WT) skin, InvEE skin, and InvEE papilloma lysates. Each track is from a different mouse. Blot probed with anti-IL1α or, as a loading control (L), β-tubulin. P: pro-IL1α; M: membrane-bound IL1α; S: soluble IL1α. (*D*) Quantitation of IL1α in skin and tumor protein lysates with cytometric beads. (*E* and *F*) Effect of Kineret on wound-induced tumor formation (*E*) and tumor incidence (*F*). F: $n = 36$ Kineret-treated (K), $n = 29$ controls (C). $^*P < 0.05$, $^{**}P < 0.01$, $^{***}P < 0.001$.

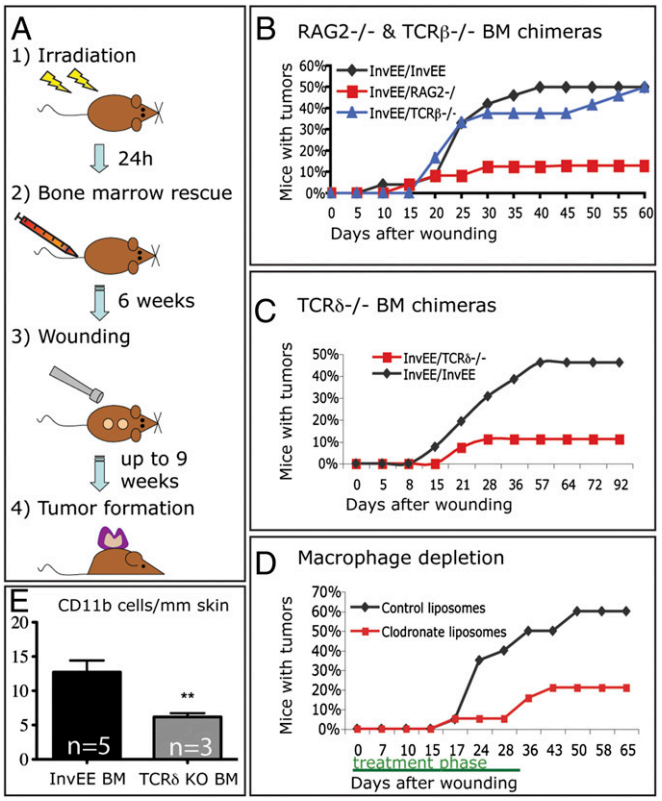

Fig. 4. Effect of bone marrow-derived cells on wound-induced tumor formation. (*A*) Schematic of bone marrow transplantation protocol. (*B* and *C*) Effect on wound-induced papilloma formation of reconstitution with Rag2 $^{-/-}$ (*B*), TCRβ $^{-/-}$ (*B*), and TCRδ$^{-/-}$ (*C*) bone marrow. (*D*) Effect of macrophage depletion with clodronate liposomes. (*E*) Number of cells expressing CD11b^{high} per millimeter of dermis in skin of InvEE mice transplanted with InvEE ($n = 5$) or TCRδ$^{-/-}$ ($n = 3$) bone marrow (BM). Unpaired t test: $t = 3.697$, $P = 0.0049$. $^{**}P < 0.01$.

reconstituted with TCRδ$^{-/-}$ bone marrow ($n = 27$) developed fewer tumors than the control group ($n = 26$; $\chi^2 = 6.17, P = 0.013$) (Fig. 4*C*). Because epidermal γδ T cells cannot be generated from adult bone marrow (17), the γδ T cells required for InvEE tumor formation must be resident in the dermis, spleen, or circulation.

We noted a reduction in CD11b-labeled monocytes in skin of InvEE mice reconstituted with TCRδ$^{-/-}$ bone marrow (Fig. 4*E*). When mice ($n = 38$) were given s.c. injections of clodronate liposomes to eliminate macrophages by induction of apoptosis (18) (Fig. S5), there was a significant reduction in wound-induced tumor formation compared with the control group injected with PBS liposomes ($n = 27$, $\chi^2 = 7.98$, $P = 0.00473$; Fig. 4*D*). We conclude that γδ T cells and macrophages are required for wound-induced papilloma formation.

Discussion

Because a hallmark of cancer is uncontrolled proliferation, it is generally assumed that tumorigenesis is initiated by dividing cells with oncogenic mutations. We show that, on the contrary, differentiated, nondividing epidermal cells with activated MEK1 can initiate benign tumor formation. Genetically normal proliferating cells and nondividing cells with an oncogenic MEK1 lesion are so fully integrated within the tumor mass that they are indistinguishable histologically (Fig. 2). The mutant differentiated cells initiate tumor formation by two processes: they recruit undifferentiated cells to form the proliferative compartment of the tumor, and they trigger an inflammatory infiltrate with tumor-promoting properties. Although the role of inflammation in tumor progression is well established, its role in tumor initiation is less well documented (8, 9).

The reduction in tumor formation that we observed on inhibition of IL1 signaling (Fig. 3) reveals a key role for IL1α. In undamaged skin, IL1α is primarily stored intracellularly; however, it is released on wounding and mechanical deformation (19, 20). As such, it is a known "alarmin," or danger factor, an endogenous molecule that signals cell and tissue damage (21). Overexpression of IL1α is not sufficient to induce skin tumors, but can accelerate tumor development under some circumstances (22). Constitutive IL1α expression can also protect against skin tumors by inducing attenuated inflammation and tumor rejection (22). However, InvEE mice do not have high serum levels of the cytokine, which may be indicative of a local, rather than a systemic, effect. In addition to inducing inflammation, IL1α release can impact on tumorigenesis by stimulating epidermal and dermal proliferation (19) and by promoting angiogenesis (23).

γδ T cells and macrophages were required for wound-induced tumor formation. γδ T cells regulate proinflammatory cytokine production by multiple immune cell subsets (24) and suppress cytotoxic T-cell activity against both tumor cells (25) and foreign antigens (26). In human burn wounds, γδ T cells hyper-activate macrophages (27), and therefore a potential role of γδ T cells in InvEE mice may be to attract macrophages (28, 29). This would be consistent with the reduction in the number of monocytes in InvEE skin following reconstitution by TCRδ$^{-/-}$ bone marrow (Fig. 4*E*). In contrast to our observations, γδ T cells protect against chemically induced skin tumors in FVB/N mice (30). This may reflect the

different mechanisms of tumor initiation: inflammation-driven versus carcinogen-driven. Furthermore, chemically induced tumors form without breaking the basement membrane; wounding may therefore represent a more physiological tumorigenic stimulus (7).

The involvement of macrophages in our model may be not only in response to γδ T cell activation, but also directly or indirectly through IL1α released by differentiating epidermal cells (31). Macrophages can have both tumor-promoting and tumor-suppressive functions, depending on the context (32). In particular, M2 polarized tumor-associated macrophages (TAMs) are known to drive tumor progression by stimulating angiogenesis and suppressing anti-tumor immunity (32, 33). In addition, clodronate liposomes are known to deplete CD11b/Gr-1–positive, myeloid-derived suppressor cells, which are important in immunosuppression and tumor promotion (18).

Our results are consistent with a model in which suprabasal activation of MEK1 leads to epidermal hyperproliferation, accumulation of IL1α, and chronic inflammation, but is not sufficient to initiate tumor formation. That occurs on wounding, when immune cells become activated through release of cytokines (such as IL-1α) or entry of pathogens. Macrophages in healing tissue are known to be M2 polarized (like TAMs), which could contribute to the protumorigenic environment (34).

Our studies reveal that nondividing, differentiated cells can initiate tumor formation by recruiting undifferentiated cells to become incorporated into the tumor and form its proliferative compartment. This highlights the limitations of cancer stem cell assays based on the ability of small numbers of disaggregated cells to proliferate in immunocompromised mice (35). Such assays overlook the contribution of differentiated cells and environmental signals such as wounding and inflammation, which can play a significant role in tumors of multilayered epithelia.

Materials and Methods

Mice. InvEE founder line 3376A mice (5) were maintained on an F1 (CBA × C57BL/6) background as heterozygotes. Transgene-negative littermates were controls. BrdU (5 mg/mL—10 μl/g of body weight) was injected 1 h before sacrifice to label S-phase cells. CAGGS eGFP mice (Jackson Laboratory) were crossed with CBA mice to create the same F1 background. Chimeras of eight-cell embryos were made as previously described (36). Rag2$^{-/-}$ (C57BL/6) mice were supplied by the Cancer Research UK Biological Resources Unit. TCRβ$^{-/-}$ (C57BL/6) mice were provided by Caetano Reis e Sousa (Cancer Research UK, London Research Institute, London). TCRδ$^{-/-}$ (C57BL/6) mice were a gift of Adrian Hayday (King's College London, London). Animal procedures were subject to Cancer Research UK ethical approval and performed under a UK Government Home Office license.

Wounding and Drug Treatments. Two separate full-thickness wounds were made in the back with a 5- or 6-mm biopsy punch (Steifel Instruments). Dexamethasone (100 μg/day; Organon), cyclosporine A (250 μg/day; Pfizer), or Kineret (15 mg/day; Amgen) was administered by one s.c. injection between the two wound sites daily for 30 d, starting the day after wounding. One hundred microliters of clodronate (gift of Roche Diagnostics, GmbH, Mannheim, Germany) or of PBS liposomes was injected s.c. adjacent to the wounds every other day, starting the day before wounding and ending 30 d after wounding.

Bone Marrow Transplantation. Allogeneic bone marrow transplants involving MHC-matched mice were performed as described (37). InvEE mice bore two MHC haplotypes: H2k and H2b. Animals used as bone marrow donors had the H2b haplotype (C57BL/6).

Sublethally irradiated (2 × 5 Gy, separated by 3 h rest) 6- to 8-wk-old InvEE females were reconstituted within 24 h by i.v. injection with 200 μL saline containing 2–5 × 10^6 male bone marrow cells freshly isolated from the tibia and femur. Chimerism was detected by Y-chromosome in situ hybridization (38).

Immunohistochemistry. The following antibodies were used: Alexafluor 647/488-conjugated anti-γδ TCR, anti-F4/80, anti-CD11b (all BD); anti-involucrin (prepared in-house), anti-GFP, anti-pH3, anti-mouse IL-1α anti-His-tag, anti-BrdU (all AbCam); anti-Ki67, anti-K14 (both Covance); and species-specific antibodies conjugated with Alexafluor 488, 555, or 647/633 (Molecular Probes).

Dewaxed paraffin sections were subjected to heat-mediated antigen retrieval (citrate buffer, pH 6) or, for eGFP detection, proteinase K digestion. Frozen sections were fixed at −20 °C in acetone or 4% paraformaldehyde for 10 min. When horseradish peroxidase (HRP)-tagged antibodies were used, sections were pretreated with 3% H_2O_2 for 5 min. Sections were blocked in 1% BSA, 10% goat or donkey serum before antibody labeling and counterstained with DAPI or hematoxylin. Images were captured with a bright field (Nikon) or confocal (Leica) microscope.

Quantitation of Ki67- and CD11b-Positive Cells. Paraffin sections of GFP/WT, GFP/InvEE skin, and GFP/InvEE papillomas were stained with antibodies to Ki67, GFP, and His tag, detected with fluorophores emitting at 633, 488, and 555 nm, respectively, and scanned with an Ariol system at 20× magnification. Cells were judged to be in the basal layer if they were in contact with the basement membrane. Ki67-positive and -negative basal cells were counted manually in at least 25 frames per sample. The total numbers of cells counted were as follows: 2,501 in GFP/WT skin, 3,425 in GFP/InvEE skin, and 4,812 in GFP/InvEE papillomas.

Frozen sections of InvEE/InvEE or InvEE/TCRδ$^{-/-}$ skin were stained with CD11b-FITC antibody and scanned as above. The number of CD11b^{high} cells in the upper dermis was counted manually and expressed per millimeter of overlying epidermis.

***TP53* and *Ha-Ras* Sequencing.** DNA was purified from papillomas using a whole-blood DNA isolation kit (Qiagen). PCR amplification of regions of interest was performed on 200 ng DNA using primers described previously (39). PCR products were purified and sequenced.

IL1α Detection. Total skin and papilloma lysates were prepared in 150 mM NaCl, 50 mM Tris-HCl, pH 7.5, 1% Nonidet P-40, 0.25% sodium deoxycholate, and protease inhibitors and subjected to Western blotting (5). IL1α levels in Nonidet P-40 lysates were analyzed using a Cytometric Bead Assay (BD Bioscience).

Statistics. Statistical analyses were performed using GraphPad Prism (GraphPad Software). Pearson's χ^2 test (two-tailed, nonparametric) was used, except when expected values were under 5, in which case a Fisher's exact test was used. Other data were analyzed with planned Student's *t* tests. *P*-values < 0.05 were considered statistically significant. To calculate 95%-confidence intervals, the Pearson–Clopper Exact method was used.

ACKNOWLEDGMENTS. We thank Caetano Reis e Souza, Adrian Hayday, Rosemary Jeffery, Manuela Ferreira, and Stephen Goldie for advice and practical help. We gratefully acknowledge Robert Rudling, Jennifer Arthur, and Cancer Research UK core resources. This work was funded by Cancer Research UK and supported by the University of Cambridge and Hutchison Whampoa Ltd.

1. Janes SM, Watt FM (2006) New roles for integrins in squamous-cell carcinoma. *Nat Rev Cancer* 6:175–183.
2. Watt FM (2002) Role of integrins in regulating epidermal adhesion, growth and differentiation. *EMBO J* 21:3919–3926.
3. Yang X, Pursell B, Lu S, Chang TK, Mercurio AM (2009) Regulation of β4-integrin expression by epigenetic modifications in the mammary gland and during the epithelial-to-mesenchymal transition. *J Cell Sci* 122:2473–2480.
4. Haase I, Hobbs RM, Romero MR, Broad S, Watt FM (2001) A role for mitogen-activated protein kinase activation by integrins in the pathogenesis of psoriasis. *J Clin Invest* 108:527–536.
5. Hobbs RM, Silva-Vargas V, Groves R, Watt FM (2004) Expression of activated MEK1 in differentiating epidermal cells is sufficient to generate hyperproliferative and inflammatory skin lesions. *J Invest Dermatol* 123:503–515.
6. Scholl FA, et al. (2007) Mek1/2 MAPK kinases are essential for mammalian development, homeostasis, and Raf-induced hyperplasia. *Dev Cell* 12:615–629.
7. Sieweke MH, Stoker AW, Bissell MJ (1989) Evaluation of the cocarcinogenic effect of wounding in Rous sarcoma virus tumorigenesis. *Cancer Res* 49:6419–6424.
8. Egeblad M, Nakasone ES, Werb Z (2010) Tumors as organs: Complex tissues that interface with the entire organism. *Dev Cell* 18:884–901.
9. Balkwill F, Charles KA, Mantovani A (2005) Smoldering and polarized inflammation in the initiation and promotion of malignant disease. *Cancer Cell* 7:211–217.
10. Sanders S, Busam KJ, Halpern AC, Nehal KS (2002) Intralesional corticosteroid treatment of multiple eruptive keratoacanthomas: Case report and review of a controversial therapy. *Dermatol Surg* 28:954–958.
11. Brown K, Buchmann A, Balmain A (1990) Carcinogen-induced mutations in the mouse c-Ha-ras gene provide evidence of multiple pathways for tumor progression. *Proc Natl Acad Sci USA* 87:538–542.
12. Kramata P, et al. (2005) Patches of mutant p53-immunoreactive epidermal cells induced by chronic UVB irradiation harbor the same p53 mutations as squamous cell carcinomas in the skin of hairless SKH-1 mice. *Cancer Res* 65:3577–3585.

13. Gurtner GC, Werner S, Barrandon Y, Longaker MT (2008) Wound repair and regeneration. *Nature* 453:314–321.
14. Stosić-Grujicić S, Lukić ML (1992) Glucocorticoid-induced keratinocyte-derived interleukin-1 receptor antagonist(s). *Immunology* 75:293–298.
15. Marionnet AV, Chardonnet Y, Viac J, Schmitt D (1997) Differences in responses of interleukin-1 and tumor necrosis factor α production and secretion to cyclosporin-A and ultraviolet B-irradiation by normal and transformed keratinocyte cultures. *Exp Dermatol* 6:22–28.
16. Lim WK, et al. (2005) Suppression of immune-mediated ocular inflammation in mice by interleukin 1 receptor antagonist administration. *Arch Ophthalmol* 123:957–963.
17. Ikuta K, et al. (1990) A developmental switch in thymic lymphocyte maturation potential occurs at the level of hematopoietic stem cells. *Cell* 62:863–874.
18. Stratis A, et al. (2006) Pathogenic role for skin macrophages in a mouse model of keratinocyte-induced psoriasis-like skin inflammation. *J Clin Invest* 116:2094–2104.
19. Robertson FM, et al. (1995) Interleukin-1α gene expression during wound healing. *Wound Repair Regen* 3:473–484.
20. Lee RT, et al. (1997) Mechanical deformation promotes secretion of IL-1 α and IL-1 receptor antagonist. *J Immunol* 159:5084–5088.
21. Bianchi ME (2007) DAMPs, PAMPs and alarmins: All we need to know about danger. *J Leukoc Biol* 81:1–5.
22. Murphy JE, Morales RE, Scott J, Kupper TS (2003) IL-1 α, innate immunity, and skin carcinogenesis: The effect of constitutive expression of IL-1 α in epidermis on chemical carcinogenesis. *J Immunol* 170:5697–5703.
23. Dinarello CA (2010) Why not treat human cancer with interleukin-1 blockade? *Cancer Metastasis Rev* 29:317–329.
24. Skeen MJ, Rix EP, Freeman MM, Ziegler HK (2001) Exaggerated proinflammatory and Th1 responses in the absence of γ/δ T cells after infection with Listeria monocytogenes. *Infect Immun* 69:7213–7223.
25. Seo N, Egawa K (1995) Suppression of cytotoxic T lymphocyte activity by γ/δ T cells in tumor-bearing mice. *Cancer Immunol Immunother* 40:358–366.
26. Xu Y, Kapp JA (2002) Gammadelta T cells in anterior chamber-induced tolerance in CD8(+) CTL responses. *Invest Ophthalmol Vis Sci* 43:3473–3479.
27. Schwacha MG (2009) Gammadelta T-cells: Potential regulators of the post-burn inflammatory response. *Burns* 35:318–326.
28. Strid J, Tigelaar RE, Hayday AC (2009) Skin immune surveillance by T cells—A new order? *Semin Immunol* 21:110–120.
29. Mantovani A, Allavena P, Sica A, Balkwill F (2008) Cancer-related inflammation. *Nature* 454:436–444.
30. Girardi M, et al. (2003) The distinct contributions of murine T cell receptor (TCR) gammadelta+ and TCRalphabeta+ T cells to different stages of chemically induced skin cancer. *J Exp Med* 198:747–755.
31. Zucali JR, et al. (1986) Interleukin 1 stimulates fibroblasts to produce granulocyte-macrophage colony-stimulating activity and prostaglandin E2. *J Clin Invest* 77: 1857–1863.
32. Allavena P, Sica A, Garlanda C, Mantovani A (2008) The Yin-Yang of tumor-associated macrophages in neoplastic progression and immune surveillance. *Immunol Rev* 222: 155–161.
33. Hagemann T, et al. (2008) "Re-educating" tumor-associated macrophages by targeting NF-kappaB. *J Exp Med* 205:1261–1268.
34. Allavena P, Sica A, Solinas G, Porta C, Mantovani A (2008) The inflammatory micro-environment in tumor progression: The role of tumor-associated macrophages. *Crit Rev Oncol Hematol* 66:1–9.
35. Gupta PB, Chaffer CL, Weinberg RA (2009) Cancer stem cells: Mirage or reality? *Nat Med* 15:1010–1012.
36. Nagy AaRJ (2000) *Gene Targeting: A Practical Approach* (Oxford University Press, New York).
37. Cui YZ, et al. (2002) Optimal protocol for total body irradiation for allogeneic bone marrow transplantation in mice. *Bone Marrow Transplant* 30:843–849.
38. Jeffery R, Poulsom R, Alison MR (2009) Sources of adult hepatic stem cells: Haematopoietic. *Methods Mol Biol* 481:141–154.
39. Niemann C, Owens DM, Schettina P, Watt FM (2007) Dual role of inactivating Lef1 mutations in epidermis: Tumor promotion and specification of tumor type. *Cancer Res* 67:2916–2921.